

Channel Measurement and Modeling in Medical Environments

Li Huang, Ruben de Francisco, and Guido Dolmans

Holst Center, IMEC-NL, High Tech Campus 31, Eindhoven, the Netherlands

Abstract

In order to facilitate the deployment of wireless systems in medical environments, channel measurements at 2.4GHz band have been performed in a hospital bedroom. Based on measurements in different line-of-sight (LOS) and non-line-of-sight (NLOS) scenarios, we determine the large-scale path loss and different small-scale fading parameters. Applying the channel models in our MATLAB simulation environment for IEEE 802.15.4 systems, we find that the simulated performance matches with our measured performance using IEEE 802.15.4 devices. This result further validates our proposed channel models.

Keywords:

Channel measurements, channel modeling, Ricean distribution

I. Introduction

Over the past years, advances in electronics and wireless communications have led to an increasing concern on the development of wireless sensor networks in medical environments [1]-[3]. To understand the performance limits of these wireless sensor networks, we need to know the characteristics of the channel, which is the wireless transmission link between the transmitter and receiver.

However, channel measurements in medical environments are still not well explored. We note that measurement results from 3.1 to 6.0GHz carried out at the Oulu university hospital for ultra wideband applications were reported in [4]. But most of the current commercialized low power wireless systems are still operating at the industrial, scientific and medical (ISM) 2.4GHz band (e.g. Bluetooth and Zigbee). Furthermore, a new 2360-2400MHz band has been proposed for new wireless medical body area network service (MBANS) and is currently under evaluation by FCC [5]. Therefore, it is important to characterize the channels around the 2.4GHz in hospitals. An intuitive solution is to use the available channel models for indoor scenarios at 2.4GHz (e.g. [6]-[8]). However, the main parameters extracted are very sensitive to the propagation environments [9]. Thus, it becomes necessary to extract the typical values of different parameters in a given medical environment.

In this paper, we present our channel measurement results at a bedroom in Kempenhaeghe Hospital, Heeze, the Netherlands.

Based on these measurements, we extract the large-scale path loss, different time dispersion parameters, and the Ricean factor that characterizes the statistical property of the amplitude variation for individual paths. To verify these extracted values, we apply the proposed channel models in a developed MATLAB simulation environment and compare the resulting simulation performance results with the experimental performance results measured from our hardware development kits. These comparison results will also be presented in the paper.

This paper is organized as follows. In Section II, we introduce our employed channel measurement technique and the considered scenarios. Then, in Section III and Section IV, we show the measurement results for large-scale path loss and small-scale fading, respectively. In Section V, by using our channel models, we present the simulation performance results and compare with the corresponding measured performance results. Finally, in Section VI, we conclude this paper.

II. Measurement Setup

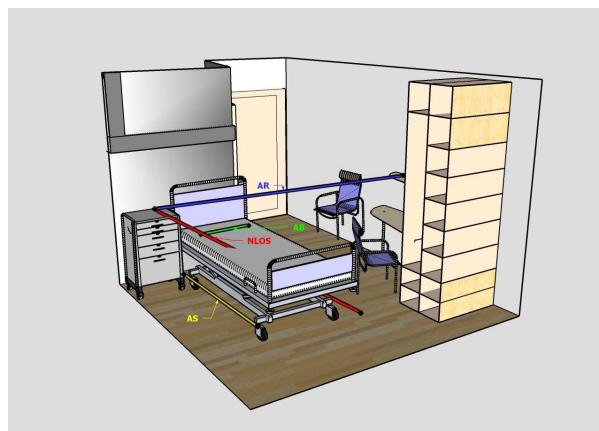


Figure 1. Channel measurements at a hospital bedroom.

A typical channel measurement technique used in indoor propagation is the frequency domain channel sounding [10][11]. This technique uses a vector network analyzer to measure the frequency domain channel. The measured frequency domain channel is then converted to the time domain channel by using the inverse discrete Fourier transform. In our

measurement, the R&S ZVL6 vector network analyzer and a 2.4GHz male Swivel antenna were used. The measured frequency range was set from 2 to 3GHz.

In this paper, we consider three line-of-sight (LOS) scenarios and one non-line-of-sight (NLOS). These three LOS scenarios include the transmission across the room (AR), transmission along the front board of the bed (AB), and the transmission along the side of the bed (AS). As illustrated in Figure 1, they are represented as the blue, green, and yellow lines, respectively. The NLOS scenario, which is represented as the red line, considers the cases where transmission is blocked by the bed. For each scenario, we fix the transmitter at the left end of each line, and move the receiver along the line to measure the channel at different distances.

III. Large-Scale Path Loss

The path loss is defined as the difference between the effective transmit power and the received power (all in dB representation). It represents the signal attenuation during transmission and is an important factor to determine the link budget analysis, which is the first step to be carried out to determine the expected system performance in a given channel scenario.

The average large-scale path loss is usually characterized as a log-distance path loss model, which is given by [11],

$$PL(d) = PL(d_0) + 10n \log(d / d_0), \quad (1)$$

where n is the path loss exponent that indicates the rate at which the path loss increases with distance, d_0 is the reference distance at which the reference path $PL(d_0)$ loss is measured. Here the path losses are represented in dB.

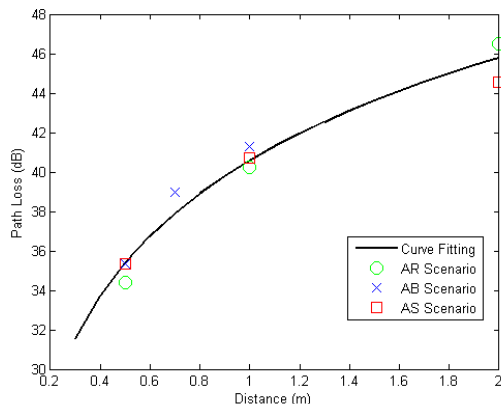


Figure 2. Path losses for different LOS scenarios and the obtained curve fitting.

A typical method to estimate n and $PL(d_0)$ from measured path losses is the linear least squares curve fitting [12]. Based on our measurement, we find that a single model suffices to represent path losses for all the three considered LOS scenarios. With this method and setting $d_0 = 1$, we obtain $n = 1.7287$, and $PL(d_0) = 40.5805$ dB. The measured path losses and the corresponding curve are shown in Figure 2. We also obtain $n = 2.4519$, and $PL(d_0) = 50.5637$ dB for the NLOS scenario.

IV. Small-Scale Fading

In the previous section, we consider the average received signal power at a given distance from the transmitter in medical environments. In this section, we consider the variability of the signal power in close spatial proximity to a particular location. This variability is called the small-scale fading, and caused by the multipath. The small-scale fading effects considered in this section include:

- Time dispersion caused by multipath propagation delays. This will be discussed in Subsection IV.1 and IV.2.
- Rapid changes in signal power over a small distance. This will be discussed in Subsection IV.3.

Note that the measured samples at a given distance are not taken in different surrounding spatial positions due to the lack of instruments that could easily control the position of antennas. Instead, we collect the samples in the frequency domain. These two set of samples are statistically identical and could be explained as follows:

The amplitudes of individual multipaths contributing to the considered multipath component normally change negligibly for a small change of distances. However, the phases of these individual multipaths change significantly, i.e. from 0 to 360 degree. Consequently, the considered multipath component might vary rapidly for a short distance. Similarly, the amplitudes of individual multipaths change negligibly, while the phases change significantly for a small change of frequency, for a small change of frequency. As a result, the effect of the change of distances is similar to that of the change of frequencies. Thus, we collect the samples in the frequency domain to resemble the samples in the spatial domain.

IV.1 Power Delay Profile

The power delay profile (PDP) gives the received power through a multipath channel as a function of time delays. It is generally represented as plots of received power as a function of excess delay with respect to a fixed time reference, which is the start of transmission in this paper.

In our measurements, we divide samples in the frequency domain into a number of groups. The adjacent samples of each group are 10MHz apart, and the frequency span is 1GHz. After applying the inverse discrete Fourier transform (IDFT), we can obtain the instantaneous power delay profile with a resolution of 1ns and the temporal span of 100ns. As the frequency domain is oversampled, we can have sufficient number of groups, each of which could resemble the set of samples in one spatial position. Thus, we could average the instantaneous power delay profiles from each group to obtain the power delay profile.

In Figure 3, we show the path losses for the worse case, i.e. NLOS scenario when the distance is 2m. From the figure, we find that the received power decreases with the transmission distance increases as expected. Further, we find that most of the energies are concentrated on a small temporal span. Even

for this worst case, the span is only within 30ns. Although not shown, similar conclusions can be drawn from other scenarios.

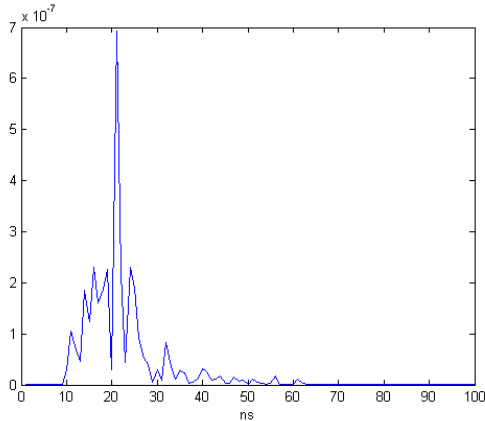


Figure 3. Power delay profile for the NLOS scenario when the distance is 2m.

IV.2 Time Dispersion Parameters

Two parameters are usually used to quantify the time dispersive properties of the channel: mean excess delay and root mean square (RMS) delay spread [11]. These delays are measured relative to the first detectable signal arriving at the receiver, and can be determined from a power delay profile discussed in the previous subsection.

Mean Excess Delay

The mean excess delay is the first moment of the power delay profile and is defined as

$$\bar{\tau} = \frac{\sum_k h_k^2 \tau_k}{\sum_k h_k^2}, \quad (2)$$

where h_k is the amplitude of the channel coefficient, and τ_k is the corresponding time delay.

We present our measured mean excess delay in different scenarios in Table 1. It shows that the mean excess delay is significantly larger in NLOS scenarios than that in the three LOS scenarios. Moreover, it shows that the mean excess delays are different in a given distance in different LOS scenarios. This is different from the large-scale path loss, which is quite similar in a given distance in different LOS scenarios. Therefore, we should differentiate the considered three LOS scenarios when we analyze small-scale fading parameters. Furthermore, we find that the mean excess delay increases with the increase of distances in LOS scenarios. This clearly indicates that the effect of multipath propagation delays becomes more significant with the increase of distances.

Table 1 - Mean excess delay in different scenarios.

Scenario	Distance (m)	Distance (m)	Distance (m)
	Mean Excess Delay (ns)	Mean Excess Delay (ns)	Mean Excess Delay (ns)

LOS/AR	0.5	1	2
	0.0337	1.1698	2.2579
LOS/AB	0.5	0.7	1
	0.7489	0.6381	1.5446
LOS/AS	0.5	1	2
	0.2024	0.8339	0.8468
NLOS	0.8	1	2
	9.3305	11.5467	10.7120

RMS Delay Spread

The RMS delay spread is the square root of the second central moment of the power delay profile and is defined as

$$\sigma_\tau = \sqrt{\frac{\sum_k h_k^2 \tau_k^2}{\sum_k h_k^2} - (\bar{\tau})^2}. \quad (3)$$

We present our measured RMS delay spreads in different scenarios in Table 2. Similar to the trends observed in the mean excess delay, it shows that the RMS delay spread is significantly larger in NLOS scenarios than that in the LOS scenarios. Again, we find that the RMS delay spread increases with the increase of distances in LOS scenarios. This further indicates that the effect of multipath propagation delays becomes more significant when the distance increases in LOS scenarios.

Table 2 - RMS delay spread in different scenarios.

Scenario	Distance (m)	Distance (m)	Distance (m)
	RMS Delay Spread (ns)	RMS Delay Spread (ns)	RMS Delay Spread (ns)
LOS/AR	0.5	1	2
	0.0337	1.1698	2.2579
LOS/AB	0.5	0.7	1
	0.7489	0.6381	1.5446
LOS/AS	0.5	1	2
	0.2024	0.8339	0.8468
NLOS	0.8	1	2
	9.3305	11.5467	10.7120

IV.3 Rayleigh and Rician Distributions

As shown in Subsection VI.1, most of the energies are concentrated on a delay spread of 30ns. Note that most of the current commercialized low power wireless systems in 2.4GHz are narrow band. For example, the chip duration of an IEEE 802.15.4 system is 500ns, which is much larger than the largest delay spread (i.e. 30ns). Thus, we can model the channel as a flat-fading channel.

From the above, the main important factor from the channel that determines the performance of an IEEE 802.15.4 system is the path loss. In Section III, we presented the results for the large-scale path loss. In this subsection, we characterize the actual path loss, which fluctuates around the large-scale path loss, due to the multipath effects. In order to get reliable statistics, we collect 3000 samples at each distance of a given scenario in the measurement.

Ricean Factor Estimation

The statistical varying nature of the received envelope of a flat-fading channel typically obeys the Rayleigh distribution or the Ricean distribution [11]. The Rayleigh distribution can be considered as a special case of the Ricean distribution when there is no stationary signal component present.

The Ricean distribution is given by

$$p(r) = \begin{cases} \frac{r}{\sigma^2} e^{-\frac{(r^2+A^2)}{2\sigma^2}} I_0\left(\frac{Ar}{\sigma^2}\right) & \text{when } A \geq 0 \text{ and } r \geq 0 \\ 0 & \text{when } r < 0 \end{cases}, \quad (4)$$

where r is the signal envelop, A denotes the peak amplitude of the stationary signal component, σ is the RMS value of the signal envelop, and $I_0(X)$ is the modified Bessel function of the first kind and zero order. The Ricean distribution is often described in terms of a parameter K , which is defined as

$$K = 10 \log \frac{A}{2\sigma^2}. \quad (5)$$

The parameter K is known as the Ricean factor and completely specifies the Ricean distribution. When K is large, the LOS component is significant. When K is small, the LOS becomes less significant. In an extreme case when K is minus infinite, the Ricean distribution degenerates to a Rayleigh distribution.

With the method proposed in [13], we obtain the estimated Ricean factors in the AR and AS scenarios as shown in Table 3. Although not shown here, in the NLOS scenario, we find that the signal envelop has a Rayleigh distribution. An interesting finding occurs in the AB scenario where there is a wall close to the transmit and receive antennas. From our measurements, similar to the NLOS scenario, we find that the signal envelop also has a Rayleigh distribution in this AB scenario. The results will be presented as a measured cumulative distribution function to be discussed later. To further analyze the effect of a wall, we consider the AR scenario when the distance is 3m. This corresponds to the situation where the receive antenna is close to the right wall as shown in Figure 1. Although not shown here, we find that the signal envelop also has a Rayleigh distribution in this situation. Thus, we may conclude that the wall will significantly contribute to the rapid change of signal power in medical environments.

Table 3 – Ricean factor in different scenarios.

Scenario	Distance (m)	Distance (m)	Distance (m)
	Ricean Factor (dB)	Ricean Factor (dB)	Ricean Factor (dB)
LOS/AR	0.5	1	2
	10.4321	4.0666	3.4102
LOS/AS	0.5	1	2
	7.3136	3.8891	3.6354

Cumulative Distribution Function

In order to further examine the statistics of the actual path loss, we compute a cumulative distribution function (CDF) based on our measured histogram. This is the measured CDF of the

path losses. It can clearly illustrate the probability of occurrences above a threshold path loss. Further, it is an efficient means to illustrate how the actual path loss deviates from the average large-scale path loss.

With the estimated Ricean factor discussed earlier, we can obtain the estimated CDF. Our results show that the estimated CDF is close to the measured CDF. Furthermore, to illustrate the effect of the wall, we plot the measured CDF for the AB scenario when the distance is 0.5m in Figure 4. Note that as the path loss instead of the signal envelop is used in the x axis in the figure, the estimated CDF is plotted as a chi-square distribution, which is equivalent to a Rayleigh distribution if the CDF of the signal envelop is used. As shown, even at this small distance, the effect of a wall still significantly affects the actual path loss since the measured CDF matches with the chi-square distribution, which suggests that this LOS scenario becomes a NLOS-like scenario whose actual path loss changes rapidly within a short distance.

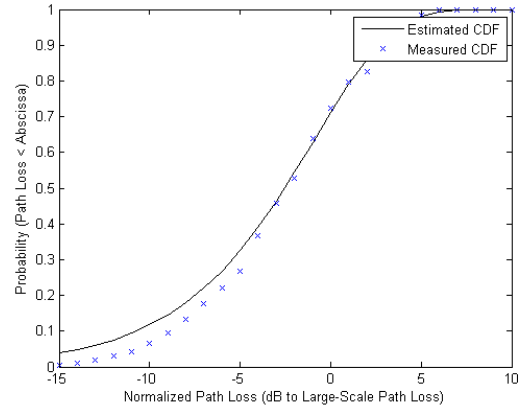


Figure 4. Measured CDF and Estimated CDF for the AB scenario when the distance is 0.5m.

V. Simulation and Measurement Results

The proposed channel models have been validated in a real scenario where several wireless devices coexist. In the performance measurement study, we use the same hospital bedroom as shown in Figure 1. Two IEEE 802.15.4 [14] enabled devices communicate, while an IEEE 802.11g [15] device interferes, thus degrading the performance in the IEEE 802.15.4 link. In order to validate the proposed channel models, a MATLAB simulator has been built that incorporates each device involved in the described communication setup, as well as the proposed channel models. Experimental results have been carried out varying the transmit power at the IEEE 802.15.4 transmitter with a fixed payload size of 10 bytes, yielding different packet error rates (PER) and RSSI measurements at the receiver.

A worst case coexistence scenario has been studied, with 100% overlap in frequency domain. While the IEEE 802.15.4 devices communicate in channel 21 (centered at 2450MHz),

the IEEE 802.11g device interferes using channel 9 (centered at 2452MHz). The interferer transmits at nominal power of 18dBm, with a heavy duty cycle of approximately 90%. Hence, transmission overlap occurs both in time and frequency domains.

The devices are distributed within the room as follows. The link between IEEE 802.15.4 transmitter and receiver is modeled as a LOS, with the devices 0.85m apart. The receiver is located on the bedside table, while the transmitter is on the bed. The link between the IEEE 802.11g interferer and IEEE 802.15.4 receiver is NLOS, with a distance of 2.5m between the devices.

As shown in Figure 5, the performance results obtained through simulations for the IEEE 802.15.4 link, using the proposed channel models, match well the measured performance obtained in the experiments. This further validates our proposed channel model.

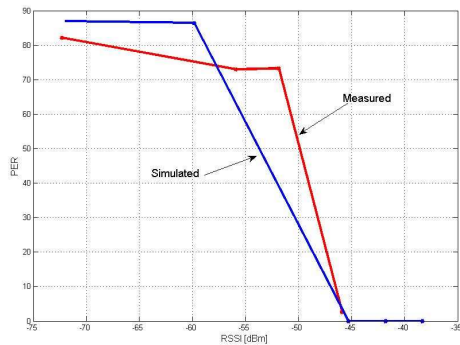


Figure 5. Simulated PER and measured PER.

VI. Conclusions

In this paper, we investigated channel characteristics in a hospital bedroom at 2.4GHz in both LOS and NLOS scenarios. We find that the delay spread of the channel is low since the channel power in all the considered scenarios is concentrated within 30ns. Although we consider three different LOS scenarios, we find a single log-distance path loss model is sufficient to characterize the large-scale path loss in these scenarios. However, the small-scale fading parameters are different in these three scenarios. We find that a wall close to the transmit and receive antennas significantly influences the variation of signal power in LOS scenarios such that signal power has a Rayleigh distribution instead of a Ricean distribution. In addition, we provide the simulation and measurement performance results. The match of these results validates our proposed channel models.

References

[1] M. Paksuniemi, H. Sorvoja, E. Alasaarela, and R. Myllyla, "Wireless sensor and data transmission needs and technologies for patient monitoring in the operating room and

intensive care unit," in *Proc. IEEE Intl. Conf. Eng. in Med. and Biol. (IEEE-EMBS)*, Shanghai, China, Sept. 2005, pp. 5182-5185.

- [2] M. R. Yuce, P. C. Ng, C. K. Lee, J. Y. Khan, and W. Liu, "A wireless medical monitoring over a heterogeneous sensor network," in *Proc. IEEE Intl. Conf. Eng. in Med. and Biol. (IEEE-EMBS)*, Lyon, France, Aug. 2007, pp. 5894-5898.
- [3] H. Fariborzi and M. Moghavvemi, "Architecture of a wireless sensor network for vital signs transmission in hospital setting," in *Proc. IEEE Intl. Conf. Convergence Inf. Technol. (ICCIT)*, Gyeongju, Korea, Nov. 2007, pp. 745-749.
- [4] L. Hentila, A. Taparungssanagorn, H. Viittala and M. Hamalainen, "Measurement and modelling of an UWB channel at hospital," in *Proc. IEEE Intl. Conf. Ultra-WideBand (ICUWB)*, Zurich, Switzerland, Sept. 2005, pp. 113-117.
- [5] <http://www.bingham.com/Media.aspx?MediaID=6965>.
- [6] S.-C. Kim, H. L. Bertoni, and M. Stern, "Pulse propagation characteristics at 2.4 GHz inside buildings," *IEEE Trans. Veh. Technol.*, vol. 45, no. 3, pp. 579-592, Aug. 1996.
- [7] E. Walker, H.-J. Zepernick, and T. Wysocki, "Fading measurements at 2.4 GHz for the indoor radio propagation channel," in *Int. Zurich Sem. Broadband Commun.*, Zurich, Switzerland, Feb. 1998, pp.171-176.
- [8] H. Zepernick and T. Wysocki, "Multipath channel parameters for the indoor radio at 2.4 GHz ISM band," in *Proc. IEEE Veh. Technol. Conf. (VTC)*, Houston, TX, May 1999, pp. 190-193.
- [9] A. Neskovic, N. Neskovic, and G. Paunovic, "Modern approaches in modeling of mobile radio systems propagation environment," *IEEE Commun. Surveys*, pp. 2-12, Third Quarter 2000.
- [10] H. Zaghoul, G. Morrison, and M. Fattouche, "Frequency response and path loss measurements of indoor channels," *Electron. Lett.*, vol. 27, no. 12, pp. 1021-1022, June 1991.
- [11] T. S. Rappaport, *Wireless communications: principle & practice*, Prentice Hall, Upper Saddle River, NJ, 1996.
- [12] D. Tummala, "Indoor propagation modeling at 2.4 GHz for IEEE 802.11 networks," M. Sc. Thesis, University of North Texas, Dec. 2005.
- [13] L. J. Greenstein, D. G. Michelson, and V. Erceg, "Moment-method estimation of the Ricean K-factor," *IEEE Commun. Lett.*, vol. 3, no. 6, pp. 175-176, June 1999.
- [14] IEEE Std 802.15.4-2006, "Wireless medium access control (MAC) and physical layer (PHY) specifications for low-rate wireless personal area networks (WPANs)," Sept. 2006.
- [15] IEEE Std 802.11g, "Wireless LAN medium access control (MAC) and physical layer (PHY) specifications: further higher data rate extension in the 2.4 GHz band," June 2003.